Heliyon 6 (2020) e04026

Contents lists available at ScienceDirect

Heliyon

journal homepage: www.cell.com/heliyon

Research article

Corrosion inhibition of brass 60Cu–40Zn in 3% NaCl solution by 3-amino-1, 2, 4-triazole-5-thiol

M. Damej [a,*], D. Chebabe [b], S. Abbout [a], H. Erramli [a], A. Oubair [b], N. Hajjaji [a]

[a] Laboratory of Materials, Electrochemistry and Environment, Team of Corrosion, Protection and Environment, Department of Chemistry, Faculty of Sciences, Ibn Tofail University, BP 133, 14000 Kenitra, Morocco

[b] Laboratory of Natural Substances & Synthesis and Molecular Dynamic, Faculty of Sciences and Techniques, Moulay Ismail University of Meknes, BP 509, Boutalamine, 52000 Errachidia, Morocco

ARTICLE INFO

Keywords:
Electrochemistry
Materials chemistry
Physical chemistry
Alloy
ATT
Isotherm
Corrosion
Zero charge potential

ABSTRACT

In this article, we tested a new organic molecule used as a corrosion inhibitor of the 60Cu–40Zn alloy in an aqueous solution similar to sea water 3% NaCl namely 3-amino-1,2,4-triazole-5-thiol (ATT) using stationary and transient electrochemical methods (polarization curves and electrochemical impedance spectroscopy (EIS)). In addition, the metal surface analysis was performed by the scanning electron microscopy (SEM) coupled with the X-ray dispersion energy (EDX) in the absence and in the presence of the inhibitor tested. Analysis of the polarization curves reveals that the ATT acts as a mixed inhibitor, while the inhibition efficiency reaches a value of 97% for a concentration of 1mM of ATT, these results are confirmed by the EIS techniques, indicating that the value of the charge transfer resistance increases with increasing of ATT concentrations, consequently the inhibitory efficiency increases and reaches a maximum value of 99% in the presence of 1mM of ATT. the influence of the immersion time shows that the corrosion inhibition of the brass 60Cu–40Zn improves with the increase of the immersion time and that the molecule adsorbs chemically and follows the Langmuir isotherm. SEM/EDS study confirms the presence of protective film on the Brass surface.

1. Introduction

Owing to particular properties, the copper and its alloys are widely used in various industrial fields, because of their interesting properties especially the high electrical and thermal conductivities; however, in the presence of oxygen, chlorides, sulphates or nitrates ions are exposed to localized corrosion [1, 2]. Some work has been done to control corrosion copper and its alloys using organic compounds that can adsorb to the metal surface to form a protective film via functional electronegative groups, electrons in conjugate bonds and heteroatom's (N, S and O) [3, 4].

Nevertheless, the use of corrosion inhibitors remains the most appropriate and practical method to ensure lasting protection against this scourge. Among the most commonly encountered inhibitors in the literature are, for example, organic compounds containing azoles rings such as benzotriazoles [5, 6], triazoles [7, 8, 9, 10], thiadiazoles [11, 12] and imidazoles [13, 14]. All these compounds showed good inhibition efficiency in 3% NaCl. On the basis of the inhibition efficiency values, the ATT has a best protective effect against corrosion of brass in 3% NaCl.

The aim of the present paper is to study the effect of the addition of 3-amino-1,2,4-triazole-5-thiol (ATT) on the corrosion resistance of Brass in 3% NaCl solution using different techniques such as potentiodynamic polarization, impedance spectroscopy and surface analysis techniques.

2. Experimental

2.1. Samples

The composition of the Brass studied was [7, 15] (wt %): 60.61 % Cu, 39.19 % Zn, 0.12 % Al, and 0.08 % Si.

2.2. Corrosion solution

The aggressive solution was prepared by dissolving sodium chloride (NaCl) in distilled water.

* Corresponding author.
E-mail address: Damejmohamed1979@gmail.com (M. Damej).

https://doi.org/10.1016/j.heliyon.2020.e04026
Received 13 December 2019; Received in revised form 29 January 2020; Accepted 15 May 2020
2405-8440/© 2020 The Authors. Published by Elsevier Ltd. This is an open access article under the CC BY-NC-ND license (http://creativecommons.org/licenses/by-nc-nd/4.0/).

2.3. Inhibitor

The organic compound tested as corrosion inhibitor is 3-amino-1,2,4-triazole-5-thiol (ATT), which is a commercial inhibitor of the "FLOKA" type, the structure of this compound, is as follows (Figure 1).

3. Methods

3.1. Potentiodynamic polarization method

The potentiodynamic polarization curves were recorded using a potentiostat PGZ101. The electrochemical measurements were performed in a conventional three electrodes electrochemical cell: Consisting of platinum electrode as Auxiliary electrode, saturated calomel electrode (SCE) as the reference and Brass alloy as the working electrode the form of a disc of the surface 0,78cm^2, the scanning speed of 1 mV/s, starting from the free potential of corrosion and moving in the cathode range towards more negative potentials until a surge of -1 V/Ag–AgCl and in the anodic domain by moving towards more and more positive potentials up to an overvoltage of 0.4 V/Ag–AgCl.

Before each measurement, the sample was polished with different grad abrasive paper (600; 1000; 1200), cleaned with acetone, washed with double distilled water and finally dried with hot air. These curves were obtained after one hour of immersion in the electrolytic solution with corrosion potential (Ecorr). Then the cathodic and anodic curves were recorded using independent plots.

3.2. Electrochemical impedance spectroscopy (EIS)

Electrochemical impedance spectra (EIS) were performed using a potentiostat PGZ 101. The design frequencies ranged from 100 kHz to 10 mHz, and these tests were conducted in an open circuit after 1 h of immersion. The data were presented as Nyquist. The inhibition efficiency (E %) was calculated using the following formula.

$$E\% = \frac{R_t^{inh} - R_t^0}{R_t^{inh}} \times 100 \quad (1)$$

Where R_t^0 and R_t^{inh} are the charge transfer resistance respectively without and with inhibitor.

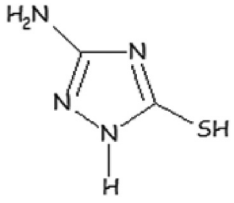

Figure 1. Chemical structure of 3-amino-1,2,4-triazole-5-thiol (ATT).

3.3. Surface analysis

The surface treatment of the alloy was carried out using a scanning electron microscopy (SEM; JEOL, JSM-IT100). After 24 h of immersion with and without inhibitor, the samples were cleaned with double distilled water and dried at room temperature. The morphology of Brass surface was examined by SEM technique.

4. Results and discussion

4.1. Polarization curves

In order to highlight the electrochemical behaviour of ATT as a cathodic, anodic or mixed type inhibitor and to elucidate its effect on kinetics of electrochemical reaction, we have drawn the brass polarization curves 60Cu–40Zn in corrosive medium both in the absence and the presence of different ATT concentrations. All polarization curves were obtained after 1 h of immersion of the metal substrate in a corrosive solution to an open circuit potential E_{corr}.

Figure 2 show typical current voltage cathodic and anodic curves obtained with and without ATT.

In cathodic field, we note that addition of the inhibitor causes a very significant decrease in the corrosion current density. It passes from the 10.68 μA.cm^{-2} without inhibitor to the 0.29 μA.cm^{-2} in the presence of 1mM of ATT. Elsewhere; we observe an appearance a pseudo-plateau who becomes wider when ATT concentration increases. For more cathodic potentials, current density increases up to a value of 1mA corresponding to the diffusion of oxygen except 1mM in ATT reaches a lower value. This behaviour can be explained by the formation of a film adhering to the surface of the electrode and do a barrier against the diffusion of oxygen.

In anodic domain, there is a displacement of the corrosion potential towards positive values indicating a slowing down of 60Cu–40Zn alloy dissolution and there is a significant decrease of anodic current density for all the ATT concentrations. This decrease is also accompanied by a change of pace with appearance of a current stage, whose current density is less than 1 μA.cm^{-2} for 0.5 mM and 1 mM ATT concentrations. The current becomes larger when ATT concentration decreases.

Electrochemical parameters issued from Figure 1 are summarized in Table 1.

The inhibition efficiency (E %) was calculated from:

$$E\% = \frac{I_{corr}^0 - I_{corr}}{I_{corr}^0} \times 100 \quad (2)$$

where I°_{corr} and I_{corr} were respectively the uninhibited and the inhibited corrosion current densities, determined by extrapolation of cathode Tafel lines to the free corrosion potential. The highest efficiency is obtained at 1 mM concentration; it reaches 97 %.

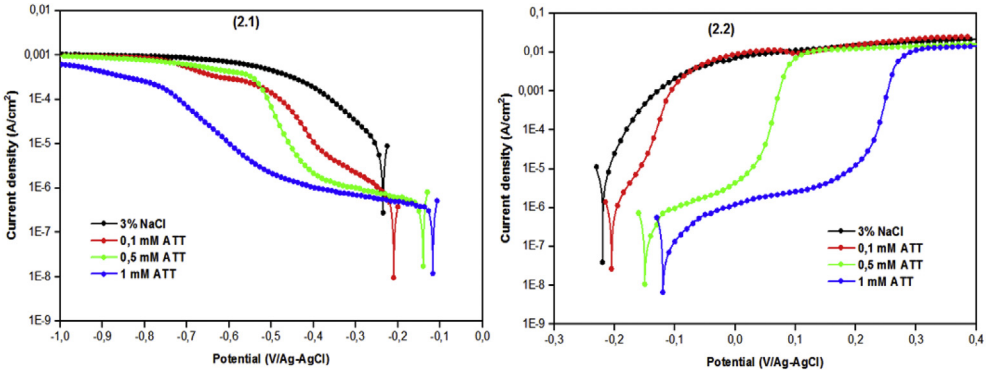

Figure 2. Cathodic (2.1) and anodic (2.2) polarization curves of brass in 3% NaCl in presence of different concentrations the ATT.

Table 1. Electrochemical parameters of 60Cu–40Zn in 3% NaCl solution without and with ATT at different concentrations.

[ATT]	Cathodic area			Anodic area			E%
	E_{corr} (mV/Ag–AgCl)	I_{corr} (μA/cm^2)	b_c (mV/dec)	E_{corr} (mV/Ag–AgCl)	I_{corr} (μA/cm^2)	b_a (mV/dec)	
0 mM	-235∓1.10	10.68∓0.05	-135∓0.85	-220∓1.06	10.35∓0.06	45∓0.20	-
0.1 mM	-207∓0.95	0.56∓0.04	-141∓0.96	-205∓1.08	0.72∓0.04	44∓0.75	94.7
0.5 mM	-141∓1.04	0.36∓0.02	-164∓0.88	-152∓1.20	0.20∓0.01	52∓0.65	96.6
1 mM	-117∓1.20	0.29∓0.01	-189∓0.75	-110∓1.03	0.10∓0.01	63∓0.80	97.3

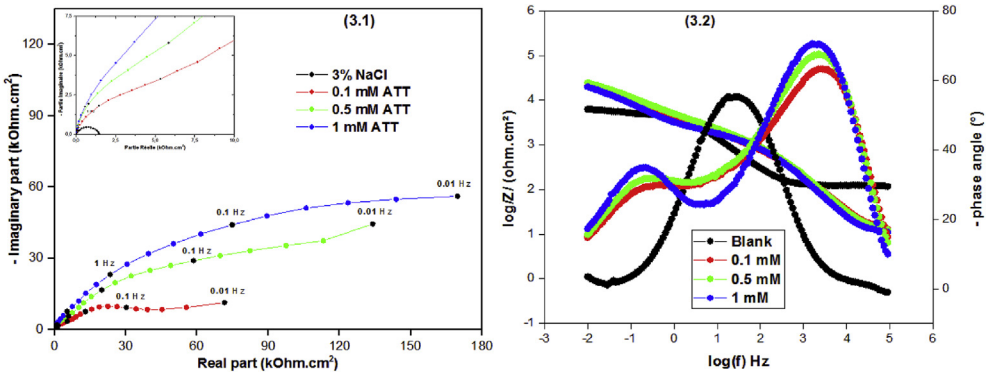

Figure 3. Electrochemical impedance (3.1) and bode (3.2) diagrams determined on 60Cu–40Zn/3% NaCl interface at different concentrations the ATT.

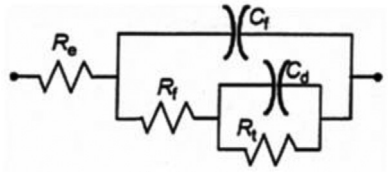

Figure 4. Equivalent electrical circuit of the metal/solution interface Electrochemical.

4.2. Electrochemical impedance spectroscopy (EIS)

4.2.1. ATT concentrations effect

The corrosion behaviour of 60Cu–40Zn brass, in 3% NaCl solution in the absence and presence of different concentrations of ATT was investigated using EIS techniques at Ecorr corrosion potential. Figure 3 shows the EIS Nyquist diagrams collected after 1 h of immersion of the Brass in the 3% NaCl solution at the free corrosion potential without and with the ATT.

In absence of inhibitor, the electrochemical impedance spectrum consists of a single capacitive loop [16].

The addition of ATT at different concentrations shows an appearance of two discernible capacitive loops with a large increase in polarization resistance, but the representation of bode clearly shows the appearance of two time constants.

At high frequencies, capacitive loop size increases with concentration, whose associated capacity values are less than 1 μF.cm^{-2} (C_f<1 μF.cm^{-2})this can be attributed to a protective film formation on the metal surface.

At low frequencies, inhibitory effect is seen by an increase of the resistance transfer value charge R_t, which show a significant variation as a function of inhibitor concentration. It reaches a maximum of the 137.23 kΩ.cm [2] with 1mM ATT concentration. The corresponding capacity decreases from 112 to 11.59 μF cm^2. These capacity values can be attributed to the ability of the double layer. According to this observation, the following electrical equivalent circuit is proposed in the Figure 4.

Parameters obtained from electrochemical impedance diagrams are summarising in Table 2.

The results recorded in Table 2 indicate that ATT effectively protects the metal surface. This is justified by an increase of the resistance transfer charge and the decrease of the double layer capacity, which are also a consequence of a progressive replacement of the vacant sites of the metallic surface by ATT, indicating decrease active sites of the dissolution reaction.

The inhibition efficiency increases with increasing inhibitor concentration, he reaches 98.97 % for 1mM ATT concentration. These results are confirmed with those found by stationary polarization curves.

Thus, the modelling of these diagrams by Ec-lab program corresponds to 2R–C circuits, this is in agreement with the results presented in reference [15, 16]. The 2R–C pairs are assigned to a contribution in descending order of frequencies to the following phenomena:

- ✓ A contribution to high frequencies (R_f–C_f) associated with dielectric character of the film formed by corrosion products reinforced by the presence of the inhibitor and ionic conduction through the pores film.
- ✓ At medium frequencies, contribution (R_t-C_{dl}) is attributed to the double-layer capacitance at 60Cu–40Zn electrolyte/brass interface at the bottom of the coupled pore of resistance transfer charge.

Table 2. Electrochemical parameters associated with impedance diagrams of 60Cu–40Zn/3% NaCl brass at different ATT concentrations.

ATT	R_f (kΩ.cm^2)	C_f (μF.cm^{-2})	R_t (kΩ.cm^2)	C_{dl} (μF.cm^{-2})	E %
0 mM	-	-	1.41∓0.02	112∓0.54	-
0.1 mM	7.47∓0.35	0.42∓0.02	37.24∓0.45	21.36∓0.87	96.21
0.5 mM	12.80∓0.55	0.25∓0.01	95.07∓0.77	16.74∓0.78	98.52
1 mM	15.84∓0.24	0.20∓0.01	137.23∓0.95	11.59∓0.54	98.97

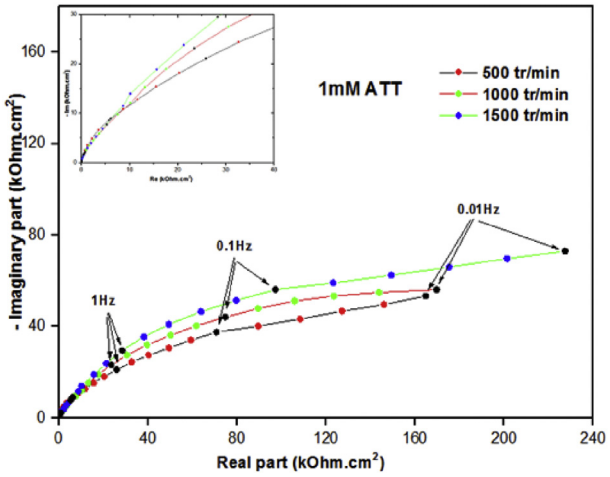

Figure 5. Electrochemical impedance diagram relating to the behaviour of brass 60Cu–40Zn at different speeds of rotation of the electrode in presence of 1mM ATT/3% NaCl.

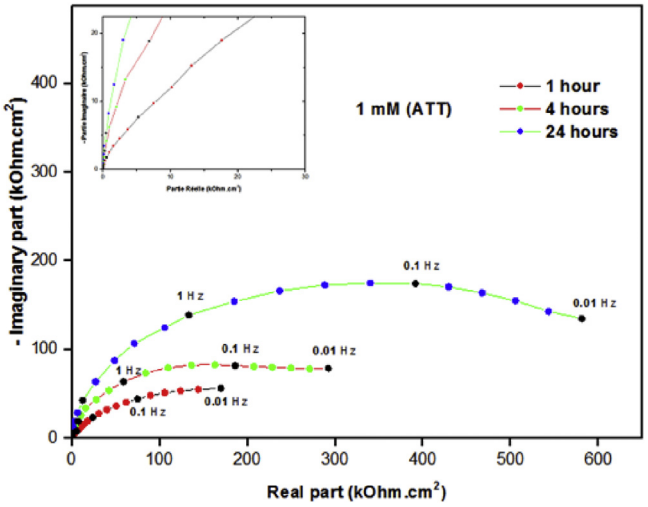

Figure 6. Effect of immersion time on impedance diagrams of the 60Cu–40Zn/3% NaCl + 1mM (ATT). Ω = 1000 rpm.

4.2.2. *Influence of rotational speed*

In order to evaluate influence of hydrodynamic conditions on inhibitory efficiency of ATT, the impedance diagrams were made at different rates of rotation of E_{corr} electrode after one hour of immersion (Figure 5).

From the form of these diagrams, it is clear that this parameter considerably conditions mass transport to the interface. The electrochemical parameters are shown in Table 3.

Analysis of this table shows that, when rotational speed increases, charge transfer resistance increases also with a decrease in the capacity of the double layer. These respective evolutions characterize on one hand, an increasing blockage of the charge transfer on the electrode surface and, on another hand, a reduction of the contact surface linked to adsorption of the inhibitor. In fact, hydrodynamic effect appears to have favoured the formation of a less permeable protective layer and having simplified the movement of mixture to the metal surface to form a layer with higher strength [17, 18, 19, 20].

4.2.3. *Effect of immersion time*

The Figure 6 shows the evolution of electrochemical impedance diagrams at corrosion potential for 1mM of ATT as a function of immersion time in a 3% NaCl solution and at a rotation speed of the electrode of 1000 rpm. The electrochemical parameters issued from the Figure 6 are summarized in Table 4.

This figure shows that the electrochemical impedance diagrams have the same shape as those obtained by concentration effect of ATT except the loop corresponding to 24 h is closed. There is also a significant increase in the polarization resistance as a function of the immersion time; it reaches a maximum of the order 153; 267.4 and 625.7 kΩ.cm [2] after respectively 1; 4 and 24 h immersion. These effects suggest that the character of inhibition of ATT results from the establishment on the brass surface a very resistant protective film that blocks corrosion process.

4.3. *Adsorption isotherm*

4.3.1. *Determination of the recovery rate*

Recovery rate θ is calculated using charge transfer resistance for different ATT concentrations at 20 °C according to the following relationship:

$$\theta = 1 - \frac{R_t}{R_t^{inh}} \tag{3}$$

R_t^{inh} and R_t are charge transfer resistance in the presence and the absence of inhibitor. Results obtained are grouped in Table 5:

Results recorded in Table 5 show that recovery rate increases when the charge transfer resistance increases.

4.3.2. *Plot of the adsorption isotherm*

A plot of C/θ versus C should yield a straight line with intercept of K^{-1}. The adsorption isotherm obtained for ATT is plotted in Figure 7.

The negative sign of free enthalpy of adsorption indicates that the adsorption of ATT at Brass surface is a spontaneous process. .The value of

Table 3. Electrochemical parameters relating to the behaviour of brass Cu–40Zn at different rotation speeds of the electrode in the presence of 1 mM ATT/3% NaCl.

Rotation speed (rpm)	R_f (kÙ. cm^2)	C_f (μF. cm^{-2})	R_t (kÙ. cm^2)	C_{dl} (μF. cm^{-2})
500	15.43∓0.47	0.20∓0.01	110.84∓0.98	14.36∓0.77
1000	15.84∓0.24	0.20∓0.01	137.23∓0.95	11.59∓0.54
1500	15.01∓0.25	0.20∓0.01	173.51∓1.15	8.02∓0.33

Table 4. Parameters determined from electrochemical impedance diagrams of interface 60Cu–40Zn/3% NaCl + 1mM ATT for different immersion times.

Immersion times	R_f (kΩ.cm^2)	C_f (μF.cm^{-2})	R_t (kΩ.cm^2)	C_{dl} (μF.cm^{-2})
1 h	15.84∓0.24	0.20∓0.01	137.23∓0.95	11.59∓0.54
4 h	23.29∓0.30	0.14∓0.01	244.11∓1.30	6.52∓0.44
24 h	42.25∓0.50	0.08∓0.00	583.50∓1.45	2.72∓0.02

Table 5. Recovery rate (θ) calculated from charge transfer resistance (R_t).

[ATT] mM	-	0.1	0.5	1
$R_t(k\Omega.cm^2)$	1.41	37.24	95.07	137.23
θ	-	0.9621	0.9852	0.9897

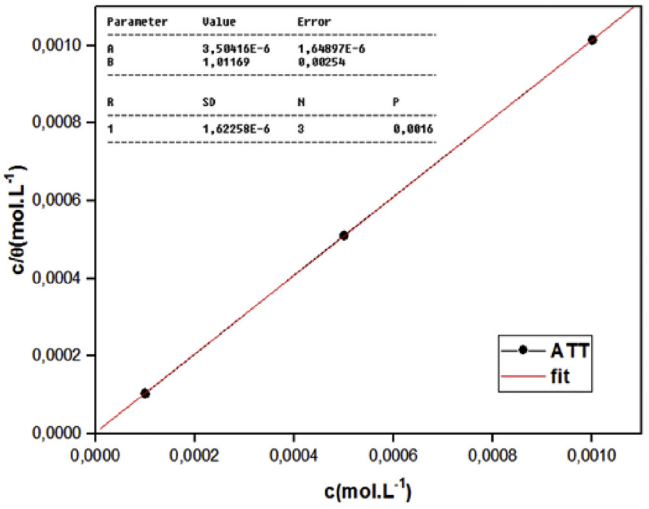

Figure 7. Langmuir adsorption isotherm model of the brass surface in 3% NaCl solution in the presence of inhibitor (ATT).

ΔG^0_{ads} is closer to -40.39 kj.mol^{-1}, and then this involves an electron transfer between the organic molecules and the metal surface. This shows that we have a chemical adsorption [21] (Table 6).

4.3.3. The zero charge potential (PZC)

Metal surface charge can be defined by the position of corrosion potential E_{corr} with respect to the zero charge potential [22, 23, 24, 25]E_{PZC}. The SIE offers a good method for determining the PZC of metals, the SIE study has been applied to different potentials and a graph of the double-layer capacitance Cdl of applied potentials is shown in Figure 8.

Table 7 shows the values of E_{corr}, E_{PZC} and E_{Γ} Zero charge 60Cu–40Zn brass surfaces at open circuit potential can be evaluated according to the equation:

$$E_{\Gamma} = E_{corr} - E_{PZC} \quad (4)$$

E_{Γ} is the rational corrosion potential as seen in Figure 8, minimum point can be called PZC of the electrode, positive values of E_{Γ} in the inhibited solution mean that surface of brass carries the positive charge in excess.

4.3.4. The inhibition mechanism

The adsorption depends also on the charge of the metal and its nature, chemical structure of the organic product and the type of electrolyte [26]. It is generally accepted that chemical adsorption process involves the transfer or sharing of electrons between inhibitor and the surface of the metal making it possible to form, respectively, coordination bonds or covalent bonds [27].

The charge transfer between metal surface and organic compound is reinforced by the presence of heteroatoms which contains pairs of free electrons. In this case, the strength of the bond established depends on the electronic density of the heteroatom and the polarizability of the functional group. In the case of aromatic compounds or unsaturated systems, the electron density will be affected by the introduction of substituents, which can increase or decrease the corrosion inhibiting efficiency. It is well known that the inhibitory action of organic compounds containing sulfur, nitrogen and/or oxygen is due to the formation of a coordination bond between the metal and the free pair of electrons present in the inhibitors [28].

The adsorption of the ATT was carried out by the free doublets of the heteroatoms of the molecule and stabilized by the aromaticity of the triazole ring (Figure 9).

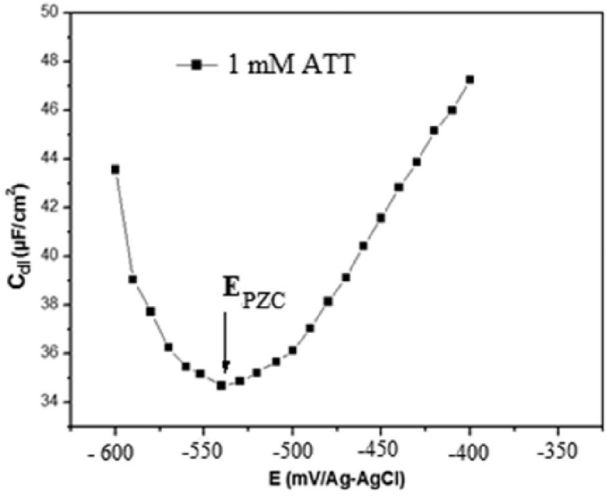

Figure 8. Differential capacitance curve in 3% NaCl + 1mM ATT solution.

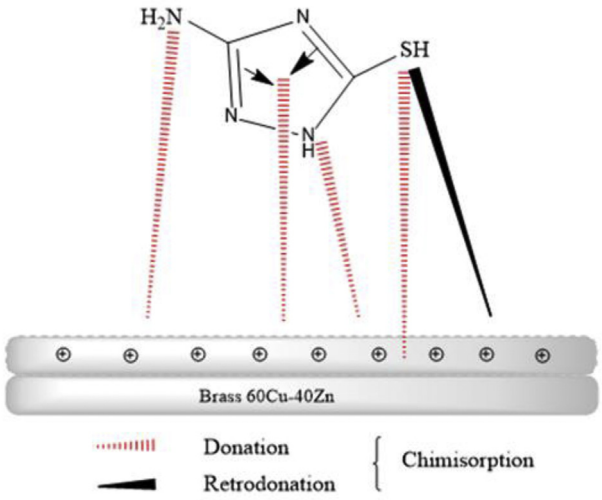

Figure 9. Graphic presentation of adsorption of 3-amino-1,2,4-triazole-5-thiol (ATT) on the 60Cu40Zn brass surface in NaCl 3% media.

Table 6. Equilibrium constant, regression coefficient and free enthalpy of adsorption of ATT on Brass in 3% NaCl.

Inhibitor	K (mol^{-1}.L)	R^2	ΔG^0_{ads} (Kj.mol^{-1})
ATT	28.69 10^4	1.00	- 40.39

Table 7. E_{corr}, E_{PZC} and E_{Γ} values recorded for 60Cu–40Zn brass in 3% NaCl solution and 3% NaCl + 1mM ATT.

	E_{corr} (mV)	E_{PZC} (mV)	E_{Γ}
1mM ATT	- 120	- 540	420

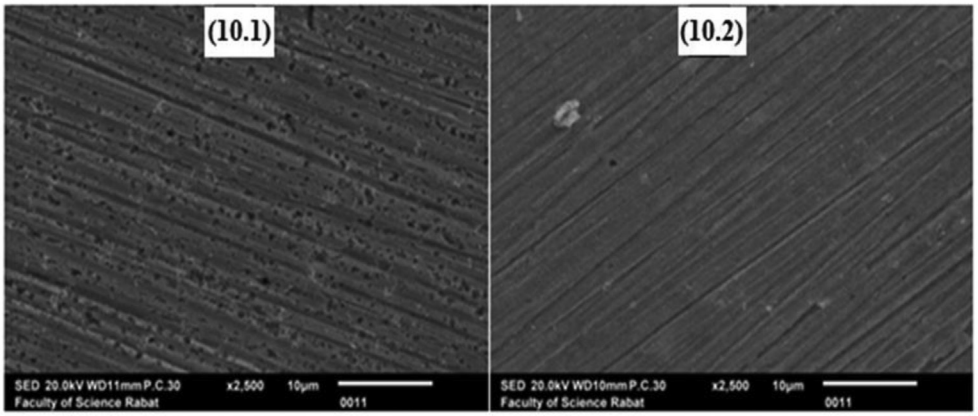

Figure 10. SEM observation of 60Cu–40Zn brass surface after 24 h of an open-circuit immersion, in the absence (10.1) and in the presence the inhibitor ATT (10.2).

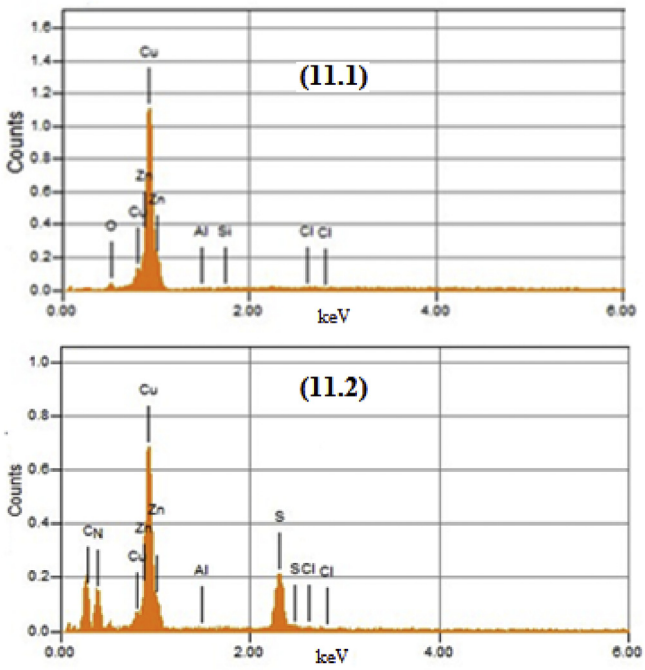

Figure 11. EDX spectrum obtained on the surface of 60Cu–40Zn brass after 24 h immersion in the absence (11.1) and in the presence the inhibitor ATT (11.2).

4.4. Surface analyses SEM/EDX

SEM photos coupled with an EDX analysis of the metal surface in the absence and in the presence of 1mM of ATT after 24 h of immersion are shown in Figures 10 and 11.

In absence of inhibitor, degradation of the surface of the alloy is noted by formation of a film formed by oxides of elements of the alloy, such as CuO, Cu_2O, CuCl and $CuCl_2$.

On the other hand, in the presence of ATT, the surface state is better preserved by the formation of a thin film visible by SEM micrograph; this result shows that ATT has an inhibitory effect on the formation of a film that has a barrier effect against aggressive ions.

Figure 10 shows the EDX analysis of the surface in the absence and the presence of the inhibitor. The spectrum has peaks attributed to carbon, nitrogen and sulphur atoms, these peaks do not appear in the case of control, so these peaks indicate the presence of an organic compound at the surface of the alloy. This results confirm the protective effect of ATT determine by the electrochemical studies.

5. Conclusions

The results demonstrated that the studied inhibitor (ATT) behaved as a promising corrosion inhibitor for 60Cu–40Zn brass in 3% NaCl solution. From the results obtained, we can conclude that:

1. Inhibition efficiency increase with increasing inhibitor concentrations to reach the maximum value of 98.97 % in the presence of 1 mM of ATT.
2. The polarization curves show that ATT is a good inhibitor for brass; it acts as a mixed type inhibitor. Thus, the electrochemical impedance measurements showed that the compound tested acts by forming an inhibitor film on the brass surface. The inhibitory properties of this film improve with the immersion time.
3. The adsorption of inhibitor follows the Langmuir isotherm and the values of the thermodynamic parameters are favourable to a chemically adsorption
4. Observation of the surface state by the SEM scanning electron microscope coupled with EDX shows the formation of an inhibitor film on the surface of the brass to act as against corrosion of this last.

Declarations

Author contribution statement

Damej Mohamed: Conceived and designed the experiments; Performed the experiments; Analyzed and interpreted the data.

D. Chebabe: Conceived and designed the experiments; Performed the experiments.

S. Abbout: Performed the experiments; Analyzed and interpreted the data.

H. Erramli: Conceived and designed the experiments; Contributed reagents, materials, analysis tools or data.

A. Oubair: Performed the experiments; Analyzed and interpreted the data; Contributed reagents, materials, analysis tools or data.

N.Hajjaji: Conceived and designed the experiments; Performed the experiments; Contributed reagents, materials, analysis tools or data.

Funding statement

This research did not receive any specific grant from funding agencies in the public, commercial, or not-for-profit sectors.

Competing interest statement

The authors declare no conflict of interest.

Additional information

No additional information is available for this paper.

References

[1] R. Vera, F. Bastidas, M. Villarroel, A. Oliva, A. Molinari, D. Ramirez, A.R. Rio, Corros. Sci 50 (2008) 729–736.
[2] A.M. Alfantazi, T.M. Ahmed, D. Tromans, Mater. Des. 30 (2009) 2425–2430.
[3] N. Dang Nam, V. Quoc Thang, N. To Hoai, P. Van Hien, Corros. Sci 112 (2016) 451–461.
[4] T. Yan, S. Zhang, L. Feng, Y. Qiang, L. Lu, D. Fu, Y. Wen, J. Chen, W. Li, B. Tan, J. Taiwan Instit. Chem. Eng. 7 (2019) 11–16.
[5] R. Ravichandran, N. Rajendran, Appl. Surf. Sci. 239 (2005) 182–192.
[6] T. Kosec, D. Kek Merl, I. Milošev, Corros. Sci 50 (2008) 1987–1997.
[7] M. Damej, D. Chebabe, M. Benmessaoud, A. Dermaj, H. Erramli, N. Hajjaji, A. Srhiri, Corrosion Eng. Sci. Technol. 50 (2015) 103–107.
[8] G. Quartarone, T. Bellomi, A. Zingales, Corros. Sci 45 (2003) 715–733.
[9] M. Benmessaoud, M. Serghini Idrissi, N. Labjar, K. Rhattas, M. Damej, N. Hajjaji, A. Srhiri, S. El Hajjaji, Der Pharma Chem. 8 (4) (2016) 122–132.
[10] O. Blajiev, A. Hubin, Electrochem. Acta 49 (2004) 2761–2770.
[11] O. Kozaderov, K. Shikhaliev, C. Prabhakar, A. Tripathi, D. Shevtsov, A. Kruzhilin, E. Komarova, A. Potapov, I. Zartsyn, Y. Kuznetsov, Appl. Sci. 9 (1-15) (2019) 2821.
[12] X. Raj, N. Rajendran, Int. J. Electrochem. Sci. 6 (2011) 348–366.
[13] H. Otmacic, E. Stupnisek-Lisac, Electrochem. Acta 48 (2003) 985–991.
[14] E. Stupnisek-Lisac, A. Gazivoda, M. Madzarac, Electrochem. Acta 47 (2002) 4189–4194.
[15] M. Damej, H. Benassaoui, D. Chebabe, M. Benmessaoud, H. Erramli, A. Dermaj, N. Hajjaji, A. Srhiri, J. Mater. Environ. Sci. 7 (3) (2016) 738–745.
[16] Z. Mountassir, A. Srhiri, Corrosion Sci. 49 (2007) 1350–1361.
[17] X. Jiang, Y.G. Zheng, W. Ke, Corros. Sci 47 (2005) 2636–2658.
[18] H. Ashassi-Sorkhabi, E. Asghari, Electrochem. Acta 54 (2008) 162–167.
[19] M. Vakili Azghandi, A. Davoodi, G.A. Farzi, A. Kosari, Corros. Sci 64 (2012) 44–54.
[20] H. Ashassi-Sorkhabi, E. Asghari, Corros. Sci 51 (2009) 1828–1835.
[21] K. Barouni, M. Mihit, L. Bazzi, R. Salghi, S.S. Al-Deyab, B. Hammouti, A. Albourine, Open. Corros. J 3 (2010) 58–63.
[22] B. Qian, J. Wang, M. Zheng, B. Hou, Corros. Sci 75 (2013) 184–192.
[23] R. Solmaz, Corros. Sci 79 (2014) 169–176.
[24] B. Xu, Y. Liu, X. Yin, W. Yang, Y. Chen, Corros. Sci 74 (2013) 206–213.
[25] B. Xu, W. Yang, Y. Liu, X. Yin, W. Gong, Y. Chen, Corros. Sci 78 (2014) 260–268.
[26] M.M. Antonijevic, S.M. Milić, S.M. Šerbula, G.D. Bogdanović, Electrochem. Acta 50 (2005) 3693–3701.
[27] G.P. Cicileo, B.M. Rosales, F.E. Varela, J.R. Vilche, Corros. Sci 41 (1999) 1359–1375.
[28] W.A. Badawy, S.S. El-Egamy, A.S. El-Azab, Corros. Sci 37 (1995) 1969–1979.